Proceedings of ASME Turbo Expo 2013: Turbine Technical Conference and Exposition
GT2013
June 3-7, 2013, San Antonio, Texas, USA

GT2013-94078

AXIAL TURBINE FLOW PATH DESIGN FOR AN ORGANIC RANKINE CYCLE USING R-245FA

Leonid Moroz
SoftInWay Inc.
15 New England Executive Park
Burlington, MA 01803, USA

Chi-Ron Kuo
Industrial Technology Research Institute
195, Sec.4, Chung Hsing Rd.
Chutung, Hsinchu, Taiwan 31040, R.O.C.

Oleg Guriev
SoftInWay Inc.
15 New England Executive Park
Burlington, MA 01803, USA

Yi-Chen Li
Industrial Technology Research Institute
195, Sec.4, Chung Hsing Rd.
Chutung, Hsinchu, Taiwan 31040, R.O.C.

Boris Frolov
SoftInWay Inc.
15 New England Executive Park
Burlington, MA 01803, USA

ABSTRACT

Limited fossil fuel resources along with the ever-increasing demand for inexpensive and environmentally friendly energy are the driving factors of geothermal and waste heat recovery technologies. In the last two decades, the Organic Rankine Cycle (ORC), has been improved and modified to better adapt the cycle to the various conditions of heat sources and has become a preferred means of exploiting low potential heat resources of various types and been widely used in many applications as an efficient and reliable energy source.

This paper represents results for the 250kW power unit, which utilizes the R-245fa refrigerant for ORC cycle in low temperature range up to 150 deg. C. The detailed design process of an ORC turbine is presented and discussed. The effect of general turbine configurations and component design on turbine efficiency and structural integrity is studied. Cost and weight cut off aspects of turbine construction also discussed. The level of efficiency achieved as a result of turbine optimization, is at the top for this class of small turbines. Final variant represents one stage axial turbine with integrally bladed disk, inlet scroll and outlet tail pipe. Structural optimization has been performed to minimize rotor weight at an acceptable level of stress and frequency safety factors.

INTRODUCTION

The Industrial Technology Research Institute (ITRI) in cooperation with the SoftInWay Inc. engineering team finished the design of a 250 kW ORC Power unit. The ITRI team mostly focused on the ORC cycle thermodynamic analysis and Power Unit components coordination and development. SoftInWay's engineering team participated in the ORC turbine development.

In this paper, we will focus on the first phase of the project - the ORC turbine design process, discussing some variants of turbine general configuration and components with regards to performance, cost/weight reduction, structural and manufacturing design criteria's. The second phase of the project is dedicated to ORC Power unit testing methodology and performance results, which will be presented in 2014.

The thermodynamic cycle of the power unit has been carried out within temperature ranges between evaporation and condensation points of 100 deg. C and 40 deg. C respectively. Based on these temperature conditions for R-245fa refrigerant real properties, performance, operation and structural requirements, all steps of ORC turbine design and analysis have been performed within the AxSTREAM software suite. Some competing variants of ORC turbine with different configurations have been developed and studied, including one stage vs. two stage configurations, unshrouded vs. shrouded blades and different meridional contour shapes. Effects of twisted vs. cylindrical blades and tip seal clearances were also evaluated with regards to efficiency and manufacturability. Integrally bladed turbine disk was considered for turbine wheel and its shape has been optimized from structural, manufacturing and material cost aspects. Additionally, aero and geometrical characteristics of the inlet scroll duct and outlet tail pipe were evaluated and modeled. Structural and modal analyses have been performed, first for preliminary geometry as part of the blade profiling and stacking process and finally for detailed geometry in 3D FEA with ANSYS and demonstrated sufficient stresses safety factors and frequency margins for integrally bladed rotor design. The final variant of turbine was selected based on complex design criteria, including performance, cost, manufacturing aspects and thrust force constraint.

NOMENCLATURE

N	power	kW
G	mass flow rate	kg/s
T	temperature	C
η_{ts}	total-to-static efficiency	-
η_{tt}	total-to-total efficiency	-

Subscripts

turb	turbine
evap	evaporator
cond	condenser

ORC CYCLE DESCRIPTION AND POWER UNIT LAYOUT

Figure 1 illustrates a Schematic diagram of an ORC system general configuration, which consists of heat supply, heat rejection, and heat conversion to power modules. The major components and their features are stated as follows. (1) Process 1-2 is the power consuming process where the liquid working fluid is pressurized by a feed pump. (2) Process 2-3 is the heat-adding process where the liquid working fluid absorbs thermal energy and vaporizes into vapor state. The heat transfer from the heat carrier fluid to the working fluid is completed via evaporators. (3) Process 3-4 is the power producing process where the heat energy of the working fluid is converted to the mechanical energy of an expander; then, an alternator converts the mechanical energy into electricity. (4) Process 4-1 is the heat-rejecting process where the vapor fluid releases heat then condenses into liquid state.

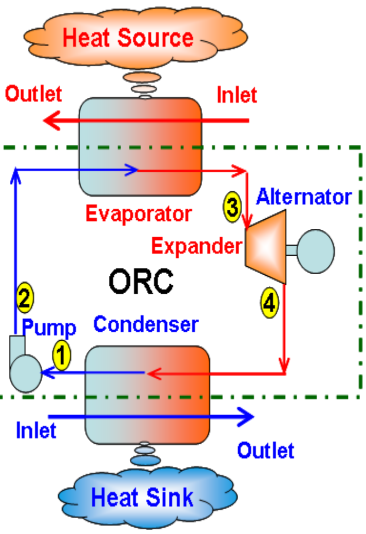

Figure 1. Schematic diagram of an ORC system

Figure 2 illustrates the thermodynamic cycle in temperature–entropy (T-s) diagram for the 250kW turbine ORC, where R-245fa is operated in sub-critical processes with $T_{evap.}$=100 deg.C, $T_{cond.}$=40 deg.C, and η_{turb}=80%. Hot water (entered the ORC at a temperature of 140 deg.C and left at 100 deg.C,) and cold water (entered at a temperature of 30 deg.C and left at 39 deg.C,) are used as heat source and heat sink, respectively. R-245fa can be categorized as dry fluid due to the slope of the saturation vapor line being positive, as shown in Figure 2. Thus, R-245fa can be set at the saturation vapor state at the turbine inlet. During and after the turbine expansion process, R-245fa would be kept at the superheated state.

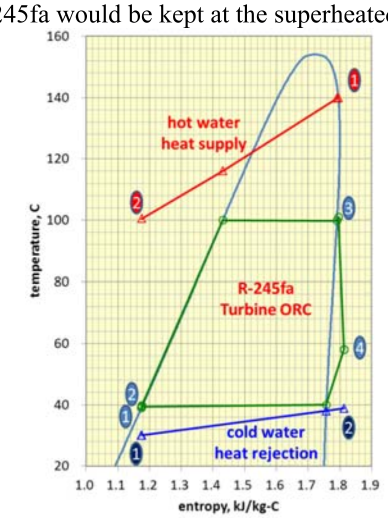

Figure 2. T-s diagram of the turbine ORC

The detailed configuration of the turbine ORC system is shown in Figures 3 and 4.

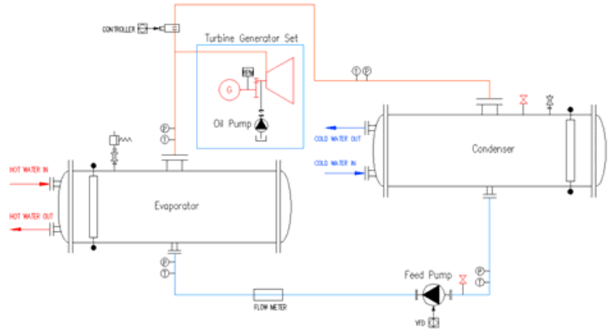

Figure 3. Configuration layout of the turbine ORC

The major components of the Power Unit are: (1) multi-stage centrifugal feed pump; (2) shell and tube evaporator; (3) axial turbine generator set; (4) shell and tube condenser. Where the turbine generator set is treated as hermetic type: all the alternator, reduction gear box, and turbine are enclosed by a casing to avoid R-245fa leakage.

Figure 4. Configuration layout of the ORC turbine

TURBINE CONFIGURATIONS ANALYSIS

Task formulation

Preliminary evaluation of an Axial vs. Radial type general configuration has been performed based on AxSTREAM design tool proven methodology ([1], [2], [3] and [5]), incorporating real R245fa working fluid properties. Performance, weight/cost and manufacturability aspects were considered in coordination with the customer and the ORC turbine general configuration has been determined as an axial with radial inflow inlet scroll duct, axial turbine, outlet tail pipe and integrally bladed disk.

To determine final turbine configuration some **design steps** were performed:

Step1. Some variants of turbine configuration were evaluated:

- number of stages – one stage vs. two stage turbine,
- meridional arrangement - constant tip diameter vs. constant mean diameter,
- shrouded vs. unshrouded blades.

Step2. Effect of tip and root seal configuration – number of teeth and radial clearance.

Based on Step1 and Step2, the final variant of general configuration was selected and next design steps were done for the final variant.

Step3. Effect of blade twist on turbine performance was studied and proper blade radial configuration was selected based on performance and manufacturing cost tradeoff.

Step4. Axial thrust analysis and design adjustment to satisfy axial thrust limitation.

Step5. Integrally bladed disk structural analyses were performed for different blisk configurations and disk shape and thickness were determined to satisfy manufacturability criteria and weight/cost of metal.

The turbine **design parameters** after ORC cycle optimization were specified as follows:

- Mass flow rate: 11.58 kg/s
- Inlet total pressure: 1260 kPa
- Inlet temperature: 101°C
- Outlet static pressure: 250 kPa
- Shaft rotational speed: 12000 rpm

A turbine isentropic efficiency higher than 80% and 250kW turbine shaft power at design point were specified as overall **design criteria.** Additional 70% turbine isentropic efficiency requirement over ±10% RPM range at off-design operation were also imposed. Turbine rotor tip diameter was limited in range from 200mm up to 400mm and inner disk diameter fixed at 50mm to match other power unit components. Axial thrust was determined as a design criterion by 4700 N to keep bearing axial load within safety limit.

Step1. General configurations and performance comparison.

The first design step was to choose a general turbine configuration. Some competing variants were generated in the AxSTREAM design tool. Three variants of high reaction turbine (~45% at mean section) with different number of stages (one vs. two) and meridional contour (constant tip vs. mean diameter) were designed and evaluated (see fig.5):

Variant 1 – one stage, constant tip diameter;
Variant 2 – one stage, constant mean diameter;
Variant 3 – two stage, constant tip diameter.

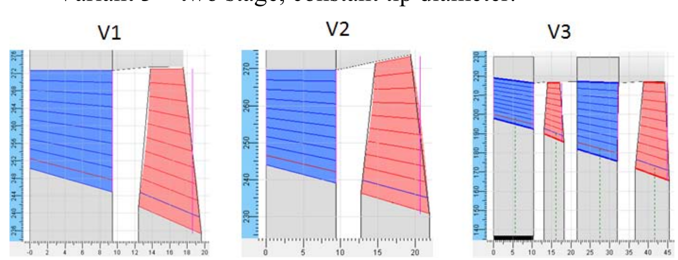

Figure 5. Three variants of general configuration

Each variant was also designed in two configurations: shrouded and unshrouded.

All 3 shrouded variants featured a labyrinth seal with 2 radial teeth. Radial tip clearance for all variants was set the same and equal to 0.25 mm with the purpose to exclude radial tip clearance impact and make results comparable. A 1D solver was utilized at this step to determine major turbine parameters and to select a variant for further design steps. In 1D solver the free vortex law assumption is used to determine tip and hub parameters and corresponding leakages. The main results of performance calculation with 1D meanline solver are presented in the table 1 below.

Table 1 – Variants performance summary

Parameter / Variant	Mass Flow, kg/sec	Power, kW	η_{ts}	η_{tt}
V1 (1 stage)	11.57	279.6	0.8082	0.8577
V1_shrouded	11.56	288.2	0.8328	0.8843
V2 (1 stage)	11.58	282.9	0.8157	0.8539
V2_Shrouded	11.57	291.3	0.8407	0.8804
V3 (2 stages)	11.59	281.9	0.8138	0.8626
V3_Shrouded	11.58	290.3	0.8382	0.8887

All variants satisfy and even exceed isentropic efficiency and power requirements. Implementation of shroud provided ~2.5% of efficiency gain. The most effective variant V2 corresponds to one stage with a constant mean diameter configuration. The two stage variant V3 with shorter blades demonstrated lower efficiency mostly because of significant influence of leakage losses in this type of turbine.

Off-design turbine performance was compared over 12000±10% rpm range. The results of calculation are presented in Figure 6 below:

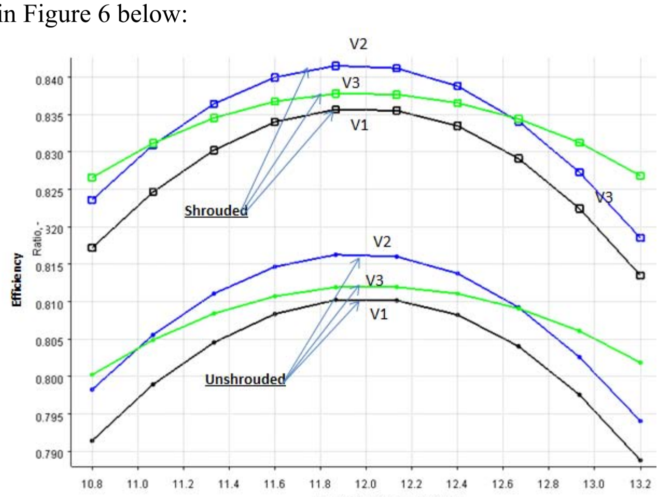

Figure 6. Off design performance comparison

All three variants demonstrated higher than the required 70% efficiency even at the furthest points of off-design modes. The 2 stage variant V3 showed lower efficiency at design point, but better performance at the furthest points because of the utilization of exit velocity from first stage by the second stage.

Step2. Leakages effect study

Additional study was performed to understand the effect of tip seal configuration – number of teeth and radial clearance - on performance. The variant V2, which demonstrated better performance among all candidates, was selected for further development and evaluated with different radial clearances. Shrouded and unshrouded variant V2 was calculated with clearances varying from 0.1 up to 1 mm. The resulting chart is presented below in Figure 7.

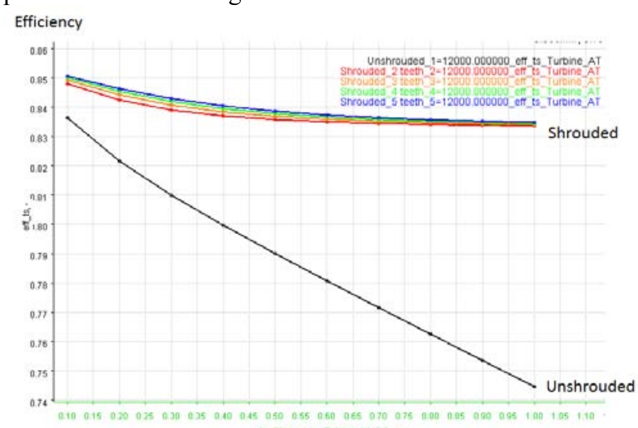

Figure 7. Influence of leakages on performance
(Black – unshrouded, Red – shrouded with 2 teeth, Orange – shrouded with 3 teeth, Green – shrouded with 4 teeth, Blue – shrouded with 5 teeth)

This chart demonstrates strong effect of tip seal configuration on performance. The most significant effect of the tip leak is observed for unshrouded blade. Each 0.1mm of clearance variation results in ~1% of efficiency change. Shrouded variant demonstrates significantly more stable efficiency vs. clearance trend but still effect of seal is important – the installation of 5 teeth instead of 2 delivered additional ~0.5% efficiency improvement.

The effect of leakages is so substantial that it was the reason why two stage variant V3 demonstrated lower efficiency in comparison with one stage variant V2. To check this effect, additional analysis was performed with second stage nozzle root clearance set to zero i.e. with no leakages in this seal (see fig. 8).

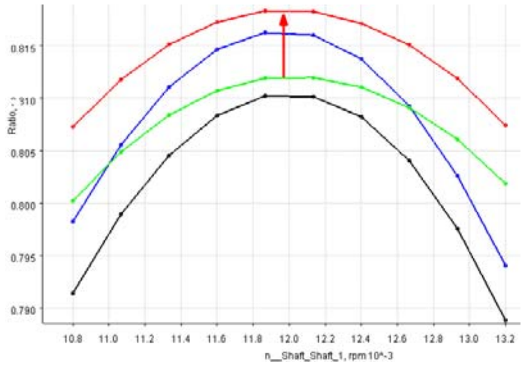

Figure 8. Total-to-static efficiency vs. shaft rotational speed (Black – V1 unshrouded, Blue – V2 unshrouded, Green – V3 unshrouded, Red – V3 unshrouded no gland seal leak)

Idealized variant V3 with zero second stage nozzle leakage demonstrates dramatically improved two stage turbine efficiency and made it the most efficient among compared variants. But with realistic second nozzle seal design this variant demonstrated lower efficiency.

Variant V2 with one stage constant mean diameter demonstrated higher performance with realistic seal design. This variant was approved by the customer and selected for further detailed development with unshrouded blades considering manufacturing and weight/cost aspects.

Step3. Evaluation of blades twist effect

During the second design step, the effect of radial parameters distribution was evaluated based on variant V2.

In this step, nozzle and blade profiling and staking process was performed, based on the radial parameters distribution obtained from the 2D solver. Twisted vs. untwisted variants of blades were evaluated and compared.

Profiling process description

To create airfoil geometry, profiles (plane sections) of each section were created using the cascade description method (Prichard method [4]).

According to this method for profile geometry, the description of the eleven parameters used are as follows:

1) Inlet metal angle - β_{1m}
2) Outlet metal angle – β_{2m}
3) Profile chord – b
4) Pitch – t
5) Throat – a
6) LE radius – r1
7) TE radius – r2
8) LE wedge angle – w1
9) TE wedge angle – w2
10) Stager angle – stgr
11) Unguided turning angle - δ_{ung}

The profiling process is made up of four main steps:

1) Find the first approximation of the stagger angle;
2) Select profile LE and TE contours to find the throat point and conjunction points;
3) Select the polynomials that best define the profile shapes; the profile is divided into three B-spline curves (pressure side spline and two suction side splines);
4) Find the polynomial coefficients to define the profile curves for the pressure side and the suction side.

Smoothness of relative velocity distribution along the pressure and suction sides and Buri criterion were controlled to ensure high efficiency and avoid flow separations. Example of profile section with velocity triangles and flow charts (velocity distribution and Buri criterion) are presented as a picture in Figure 9 below.

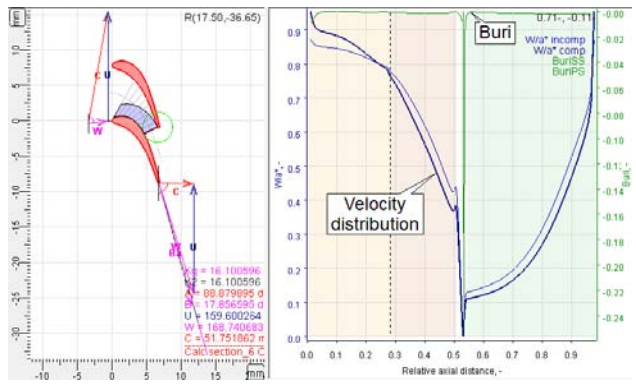

Figure 9. Meanline profile section and flow charts

The twisted vs. untwisted airfoils performance analysis.

The AxSTREAM design system provides the ability to create 3D twisted airfoils with any complicated geometry such as sweep, lean, and bow. Two configurations for nozzles and blades design - twisted vs. cylindrical (constant profile) airfoils - were designed for all 3 variants. See figure 10 below.

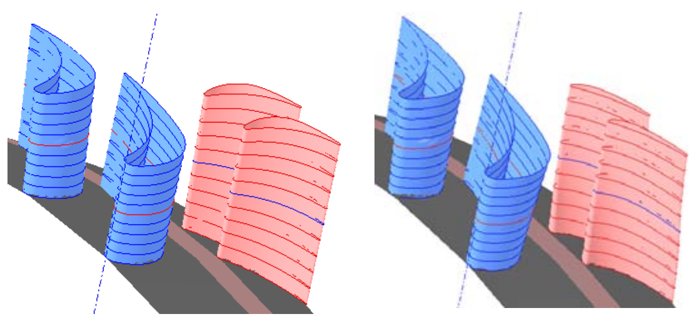

Cylindrical profiles Twisted airfoils

Figure 10. V2 cylindrical and twisted airfoils

Performance comparison from 2D solver for design point operation demonstrated ~ 1-1.5% of efficiency shortfall resulting from cylindrical blades, compared to twisted - see table 2 below.

Table 2 – Twisted vs. Cylindrical performance summary

Parameter / Variant	Mass Flow, kg/sec	Power, kW	η_{ts}	η_{tt}
V1	11.57	279.6	0.8082	0.8577
V1_cylindrical	11.61	275	0.7911	0.8406
V2	11.58	282.9	0.8157	0.8539
V2_cylindrical	11.61	280.9	0.8075	0.8484
V3	11.59	281.9	0.8138	0.8626
V3_cylindrical	11.62	278.9	0.8020	0.8505

Additional losses resulted from high incidence angles that appeared on blade because of constant inlet metal angles. Figure 11 below represents radial angles distribution for both configurations and significant difference for blade incidence angles.

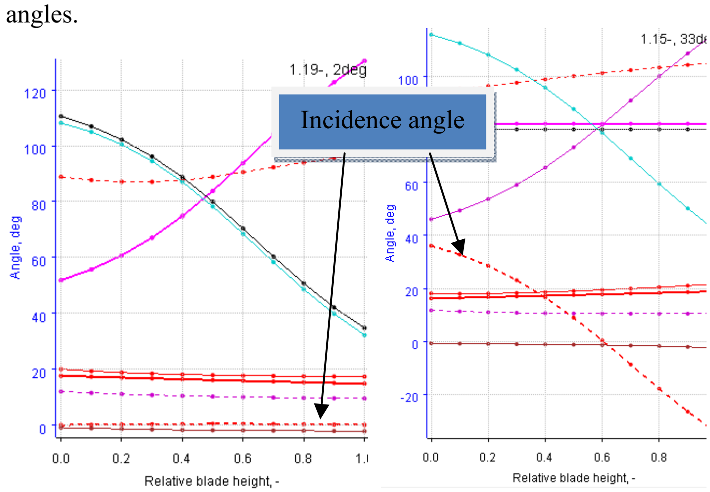

Twisted airfoil Untwisted airfoil

Figure 11. Incidence angles comparison

The incidence angles that appeared on cylindrical blade varied from 36.1° at hub up to –34.4° at tip radius. This comparison clearly demonstrates advantages of twisted configuration over cylindrical in turbine performance, but results in higher manufacturing cost.

FINAL VARIANT SELECTION

Based on Step1, Step2 and Step3 performance analyses and considering manufacturing and weight/cost aspects the final variant selection was chosen after discussion with customer in favor of untwisted and unshrouded blades variant V2.

Step4. Axial thrust limitation satisfaction

Axial thrust was calculated for second variant V2 as the most efficient among the three candidates studied. Axial thrust value for V2 with high mean reaction and without balance holes was 13079N. High axial thrust values were caused by the large pressure difference acting on the rotor occurring due to the stage's high reaction. Pressure in upstream disk chamber was ~0.427 MPa and in downstream disk chamber ~0.25 MPa.

The calculated value of the axial thrust significantly exceeded the specified design limit of 4700N.

To reduce thrust to the required level, two variants of the turbine design were evaluated. First design assumed disk balance holes and second assumed lower reaction.

An analysis of turbine performance with balance holes was performed in the design software tool with the purpose of determining a sufficient holes configuration. The addition of balance holes in variant V2 helped to decrease axial thrust value to the required 4645N but at the cost of a 3.2% efficiency shortfall.

Variant V4 turbine with lower reaction (~28% at mean section instead of 45% at preliminary steps) inherited V2 main features and was designed to decrease pressure drop on blades and disk. Pressure in the upstream disk chamber dropped from ~0.427 MPa to ~0.3 MPa and in downstream disk chamber it remains equal to ~0.25 MPa. Variant 4 with lower reaction helped to satisfy axial thrust requirements and obtain higher efficiency comparing to variant V2 with balance holes. Performance and thrust data are presented in table 3 below

Table 3 – Comparison of integral performance

	V2	V2 BH	V4 low react
Axial thrust total, N	13079	4649	4434
Axial thrust blades, N	4029	3599	1853
Axial thrust disk, N	9050	1050	2581
Total to static efficiency, -	0.8075	0.7838	0.7949

Final performance evaluation was done for variant V4 in Figure 12 below accounting for the additional losses at inlet duct and effect of pressure recovery at exhaust diffuser. With 2% of pressure loss at the turbine inlet and pressure recovery effect in outlet diffuser, total-to-static efficiency of the selected variant V4 was evaluated as 81.8% at design point operation and satisfied off-design efficiency requirement.

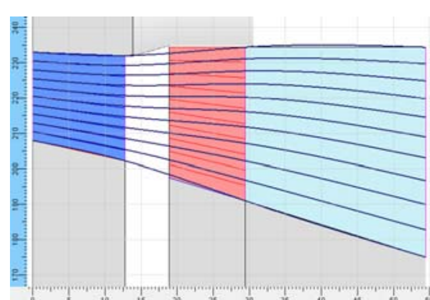

Figure 12. Final variant flow path shape after streamline calculation

It is worth mentioning that a significant impact on performance improvement was achieved by means of pressure recovery in the exhaust diffuser. The ~ 3% efficiency increase resulted from stage heat drop growth due to pressure recovery effect in the outlet duct.

MECHANICAL DESIGN

3D solid modeling was completed before final Step5 – detailed design structural evaluation.

Final variant 3D solid model with turbine flowpath, inlet and outlet components presented at Figure 13.

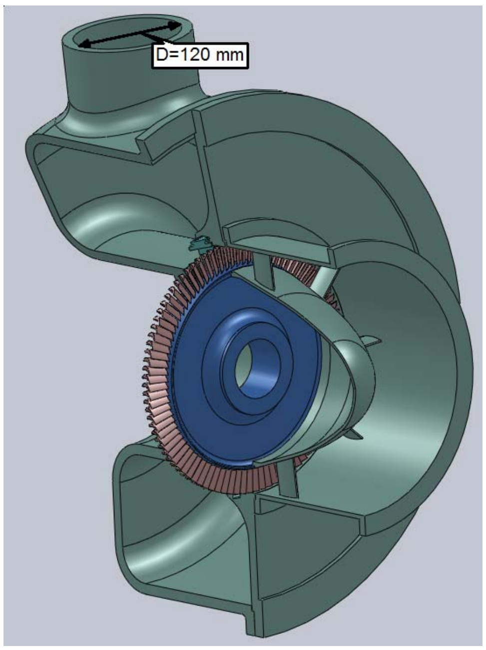

Figure 13. Final variant 3D solid model.

Step5. Mechanical design and structural analyses.

At this step detailed mechanical design and structural analyses were performed to determine the final disk configuration. Some variants of an integrally bladed disk with different thicknesses were considered and structurally evaluated. The objective of this step was to determine the final disk configuration, satisfying stress and frequency safety factors and also manufacturability aspects.

Stress and modal analysis under centrifugal and bending loads was performed in 3D FEA ANSYS [6].

A blisk inner diameter of 50 mm was determined as a design criterion. Blisk hub thickness and width were designed to transfer torque from disk to shaft with a dowel. Disk neck was the only varied parameter to determine final geometry and two variants with thicknesses of 4mm and 6 mm were studied in the final configuration.

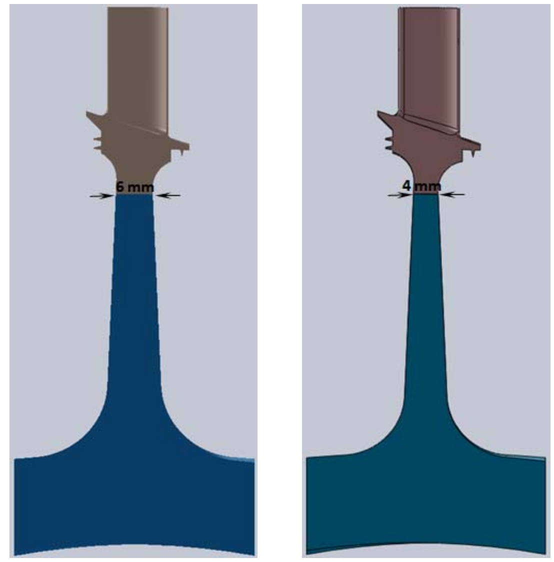

Figure 14. 2 Blisk models with two different neck thicknesses

Von Mises stresses distribution for both variants is presented in Figure 15. Disk average stress distribution is presented in Figure 16 and demonstrates sufficient safety factor for both variants.

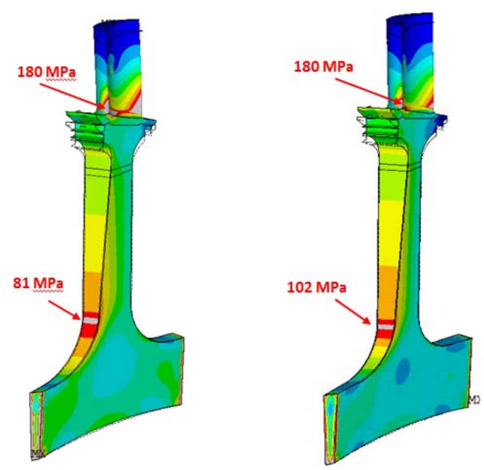

Figure 15. 2 Blisk von Mises stress distribution

The safety factor for both variants was higher than the specified allowable stress limit of equal 2.0. Local stress

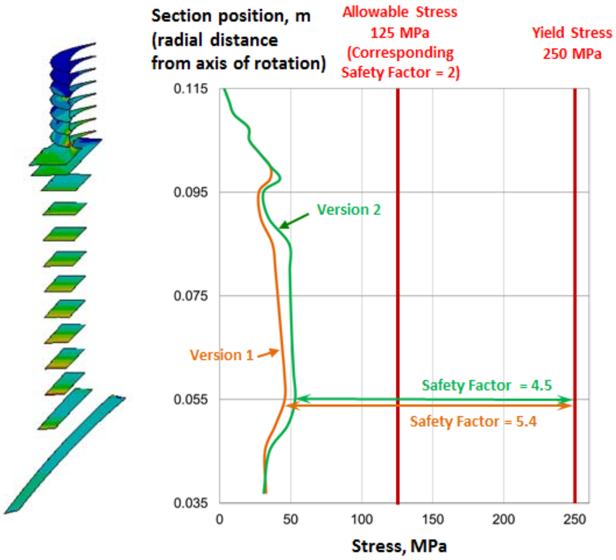

Figure 16. 2 Blisk von Mises average stress spanwise distribution

Maximal local stress ~ 180 MPa observed at blade root zone and ~ 100 MPa at disk fillet are significantly below yield stress limit.

Modal analysis results are presented in Figure 17 and demonstrated sufficient separation margins for rotational frequency at 12 nodal diameters (ND) and nozzle passing frequency.

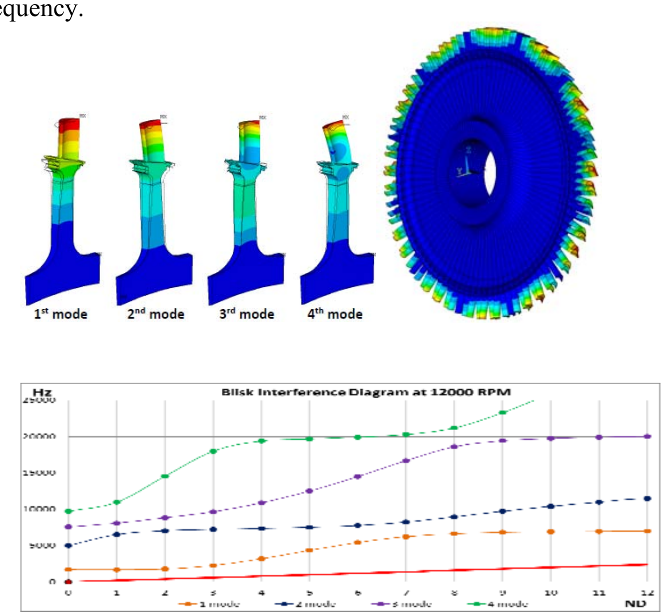

Figure 17. Blisk modal analysis results:

- first 4 mode shapes for blisk sector;
- first modal shape for full blisk 6ND;
- blisk interference diagram for 12 ND;

After consultation with customer and taking into account aspect of blisk manufacture it was decided to proceed with 6 mm disk neck thickness.

CONCLUSIONS

Ever increasing fuel costs and limited fossil fuel resources are significant driving factors of the increasing demand for green energy solutions. This article represents the results of an ORC unit design and focuses on turbine details related to the turbine flow path, aerodynamic and structural design and highlights some of the key factors affecting final configuration decisions.

The effect of turbine general configurations and component design on turbine efficiency and structural integrity is studied. Cost/weight aspects of turbine construction play a significant role in the final variant selection. The level of efficiency achieved as a result of turbine flowpath optimization, is at the top for this class of small turbines (81.7%). Final variant represents a 1 stage axial turbine with integrally bladed disk (blisk), inlet scroll and outlet tail pipe. Turbine flow path with mid reaction level was selected due to limitations on axial thrust. Structural analysis has been performed to understand the effect of disk geometry and achieve acceptable stresses and frequencies safety factors.

The designed power unit is planned to be manufactured and tested in 2013. The performance comparison of the test results with 1D and 2D calculations will be presented in the paper at ASME Turbo Expo 2014.

REFERENCES

[1] Moroz L., Govorushchenko Y., Pagur P., 2006, A Uniform Approach to Conceptual Design of Axial Turbine/Compressor Flow Path, Future of Gas Turbine Technology, 3rd International Conference, Brussels, Belgium

[2] H. R. M. Craig, H. J. A. Cox, "Performance Estimation of Axial Flow Turbines". The Sust. Of Mech. Eng/ Proc, 1970/71, vol. 185, 32/71, P. 407-424

[3] Aungier R.H., "Turbine Aerodynamics: Axial-Flow and Radial-Flow Turbine Design and Analysis", ASME Press, 2006

[4] Pritchard, L. J., "An Eleven Parameter Axial Turbine Aerofoil Geometry Model", ASME Paper 85-GT-219, 1985

[5] Leonid Moroz, Yuri Govorushchenko, Petr Pagur, "Axial Turbine Stages Design. 1D/2D/3D Simulation, Experiment, Optimization", ASME Turbo Expo 2005: Power for Land, Sea and Air, GT2005-68614.

[6] ANSYS Inc., Mechanical APDL, Release 14 Preview.